PNAS RESEARCH ARTICLE | NEUROSCIENCE OPEN ACCESS

High-performance optical control of GPCR signaling by bistable animal opsins MosOpn3 and LamPP in a molecular property–dependent manner

Mitsumasa Koyanagi[a,b,c,1,2], Baoguo Shen[c,1], Takashi Nagata[c], Lanfang Sun[c], Seiji Wada[a], Satomi Kamimura[c], Eriko Kage-Nakadai[b,d], and Akihisa Terakita[a,b,c,2]

Edited by Paul Sternberg, California Institute of Technology, Pasadena, CA; received March 11, 2022; accepted October 5, 2022

Optical control of G protein-coupled receptor (GPCR) signaling is a highly valuable approach for comprehensive understanding of GPCR-based physiologies and controlling them precisely. However, optogenetics for GPCR signaling is still developing and requires effective and versatile tools with performance evaluation from their molecular properties. Here, we systematically investigated performance of two bistable opsins that activate Gi/Go-type G protein (mosquito Opn3 (MosOpn3) and lamprey parapinopsin (LamPP)) in optical control in vivo using *Caenorhabditis elegans*. Transgenic worms expressing MosOpn3, which binds 13-*cis* retinal to form photopigments, in nociceptor neurons showed light-induced avoidance responses in the presence of all-*trans* retinal, a retinal isomer ubiquitously present in every tissue, like microbial rhodopsins and unlike canonical vertebrate opsins. Remarkably, transgenic worms expressing MosOpn3 were ~7,000 times more sensitive to light than transgenic worms expressing ChR2 in this light-induced behavior, demonstrating the advantage of MosOpn3 as a light switch. LamPP is a UV-sensitive bistable opsin having complete photoregenerative ability by green light. Accordingly, transgenic worms expressing LamPP in cholinergic motor neurons stopped moving upon violet light illumination and restored coordinate movement upon green light illumination, demonstrating color-dependent control of behavior using LamPP. Furthermore, we applied molecular engineering to produce MosOpn3-based tools enabling light-dependent upregulation of cAMP or Ca^{2+} levels and LamPP-based tool enabling clamping cAMP levels color dependently and context independently, extending their usability. These findings define the capacity of two bistable opsins with similar retinal requirement as ChR2, providing numerous strategies for optical control of various GPCR-based physiologies as well as GPCR signaling itself.

rhodopsin | second messenger | cAMP | Ca^{2+} | signal transduction

G protein–coupled receptors (GPCRs) are transmembrane receptors, which are involved in various cellular and physiological functions including neural responses, cell metabolisms, and hormonal responses (1, 2). GPCRs generally bind a variety of chemical ligands such as odorants, hormones, and neurotransmitters and transduce these extracellular signals into intracellular responses (GPCR signaling) via heterotrimeric G proteins. The GPCR signaling varies mainly depending on the subtype of G protein alpha subunit engaged and includes upregulation and downregulation of cAMP, by Gs- and Gi-type G proteins, respectively, and phosphoinositol signaling for Ca^{2+} elevation mediated by Gq-type G protein. Most animals have hundreds of GPCR genes, and humans, for example, have ~800 GPCR genes, indicating the importance of GPCR signaling for biological activities (3). Although the structure–function relationships of many GPCRs have been well investigated so far, for comprehensive understanding of GPCR-based physiologies as well as controlling them precisely, optical control of GPCR signaling would be one of the ultimate approaches because of high temporal resolution of light stimulus.

Animal rhodopsins (opsin-based pigments), which underlie vision and nonvisual functions such as circadian photoentrainment in varied animals, consist of a protein moiety, opsin, and a chromophore (11-*cis* retinal in many cases) and basically serve as light-sensitive GPCRs (4). Therefore, opsins have been considered promising tools for optical control of GPCR signaling, and indeed, such optogenetic application has succeeded to some extent using vertebrate visual opsins (5–7). However, the fact that relatively small number of papers on optogenetic research using animal opsins have been published until now compared with that using microbial rhodopsins such as ChR2 for optical control of neural activities suggests that there is still room for improvement. The point would be related to molecular properties of vertebrate visual opsins: 1) they basically form photopigments by binding to 11-*cis* retinal, which is abundant in photoreceptor tissues like the eyes but not

Significance

Optogenetics for GPCR signaling is highly valuable but is still developing and requires effective tools like ChR2. We demonstrated that two animal opsins, mosquito Opn3 (MosOpn3) and lamprey parapinopsin (LamPP), are available in optogenetics equivalently to ChR2 in terms of retinal requirement. Furthermore, MosOpn3 introduced into nociceptor neurons of *C. elegans* exhibited ~7,000 times higher sensitivity than ChR2 in the light-induced avoidance behavior. LamPP introduced into motor neurons induced violet light-dependent stop and green light-dependent go, demonstrating color-dependent control of behavior using LamPP. In addition, our molecular engineering extended the usability of MosOpn3 and LamPP to different signaling cascades and kinetics. The current findings provide numerous strategies for optical control of various GPCR-based physiologies as well as GPCR signaling itself.

Author contributions: M.K. and A.T. designed research; M.K., B.S., T.N., L.S., and S.K. performed research; M.K., B.S., T.N., L.S., S.W., S.K., E.K.-N., and A.T. contributed new reagents/analytic tools; M.K., B.S., T.N., S.W., S.K., E.K.-N., and A.T. analyzed data; and M.K. and A.T. wrote the paper.

The author declares no competing interest.

This article is a PNAS Direct Submission.

[1]M.K. and B.S. contributed equally to this work.

[2]To whom correspondence may be addressed. Email: koyanagi@omu.ac.jp or terakita@omu.ac.jp.

This article contains supporting information online at https://www.pnas.org/lookup/suppl/doi:10.1073/pnas.2204341119/-/DCSupplemental.

Published November 23, 2022.

in other tissues (11-*cis* retinal requirement), and 2) after light absorption, their photoproducts immediately release chromophore (bleach) to be functionless (bleaching property), both of which are unfavorable characteristics for high-performance optical control of GPCR signaling, especially in vivo (4). To overcome the problems associated with the molecular properties, utilization of animal opsins that is more suitable for optogenetic tools should be required.

To date, thousands of opsins have been identified from a wide range of animals from cnidarians to vertebrates, and they are phylogenetically divided into eight or more groups, which is almost consistent with the classification based on G protein selectivity and activation manner (4, 8). With respect to the photochemical property, opsins are basically classified into two types: bleaching opsins like vertebrate visual opsins and bleach-resistant or bistable opsins, which convert to stable active states upon light absorption, and in many cases, the active states revert to the original inactive state by subsequent light absorption (4, 9), like invertebrate visual opsins (10–13). The bistable nature appears to be suitable for sustained optical control of GPCR signaling. In fact, a bistable opsin melanopsin (OPN4) was applied to optical control of some physiologies including restoration of vision (14–16). In addition to melanopsin, we have identified many kinds of bleach-resistant/bistable opsins from both invertebrates and vertebrates (10, 17–23). Among them, we particularly focused on optogenetic potentials of Opn3 and parapinopsin because of their interesting molecular properties, which are recently receiving increasing attention (24).

Opn3 was first identified from the mammalian brain and therefore originally called encephalopsin (25). Then, its homologues were identified from many animals and revealed to be expressed in their various tissues including the brain, suggesting their involvement in photoreception in "nonphotoreceptive" tissues. We have previously succeeded in functional analyses of members of the Opn3 group (22, 26) and found that one of the members mosquito Opn3 (MosOpn3) has a unique property; it forms a photopigment that light dependently activates Gi- and Go-type G proteins when bound to 13-*cis* retinal as well as 11-*cis* retinal (22, 27). Since 13-*cis* retinal is thermally equilibrated with all-*trans* retinal, a retinal isomer ubiquitously present in animals, we have proposed the idea that the Opn3 is applicable to anywhere in the body as an optogenetic tool. In fact, mammalian cultured cells expressing the MosOpn3 exhibited a light-induced decrease in the intracellular cAMP level probably mediated by the Gi activation with all-*trans* retinal addition or even without retinal addition in the presence of only a small amount of retinoid in the serum (22). The idea was also supported by a recent report showing optogenetic silencing of neurotransmitter release with the MosOpn3 in vitro and in vivo (28).

Another promising bistable opsin parapinopsin was first identified from catfish pineal and parapineal organs (29) and thereafter from many lower vertebrate pineal-related organs (17, 23, 30, 31). Spectroscopic and biochemical analyses revealed that the lamprey parapinopsin (LamPP) is an ultraviolet (UV)-sensitive bistable opsin, which activates transducin and Gi-type G protein upon UV light absorption (32–34). Notably, parapinopsins convert to a stable active state having an absorption maximum at ~500 nm (in the green region), which is largely distinct from that of the inactive dark state (32). The large spectral difference between the inactive and active states allows selective illumination of the active state, resulting in its complete recovery to the inactive state (17). The same is true for the signal transduction level. The G protein activation by parapinopsin was up- and down-regulated by UV and green light illumination, respectively, in vitro and in vivo (33–38), demonstrating its optogenetic potential for color-deendent on and off of GPCR signaling.

Here, to evaluate performances of MosOpn3 and LamPP in optical control of GPCR signaling in vivo based on their molecular properties, we focused on *Caenorhabditis elegans*, in which the relationships between GPCR signaling and behaviors have been well defined. Importantly, in the case of optogenetics in *C. elegans*, isomeric forms of chromophore retinal can be controlled by exogenously adding specific retinal isomers (6, 39), which is an irreplaceable advantage in testing the chromophore requirement of opsin for functioning in vivo, in 11-*cis* form poor condition. In this paper, we showed that MosOpn3 functions in vivo under the absence of 11-*cis* retinal with much higher sensitivity compared with ChR2, which is the most used optogenetic tool. We also succeeded in color-dependent control of *C. elegans* behavior using LamPP. Together with our demonstration of introducing G protein selectivity of particular GPCRs into MosOpn3 and LamPP, the current findings provide versatile and powerful optogenetic tools for controlling GPCR signaling and various physiologies based on the molecular properties of the two opsins.

Results

Optical Control of *C. elegans* Behavior Using the Mosquito Opn3. We evaluated the performance of mosquito Opn3 (MosOpn3) for its molecular property–based optical control of GPCR signaling in vivo using *C. elegans*. Since MosOpn3 is a Gi/o-coupled opsin (22), we focused on ASH neurons, a kind of nociceptors, in which chemoreceptors trigger Gi/o-like G protein (ODR-3)–mediated signal transduction upon ligand binding to induce avoidance behavior of *C. elegans* (40, 41) (Fig. 1*A*). MosOpn3 was introduced into ASH neurons under the control of the *sra-6* promoter, a chemosensory receptor mainly expressed in ASH neurons (42) (Fig. 1*B*). We obtained several lines of transgenic (Tg) worms that express MosOpn3 in ASH neurons (MosOpn3-worms) with the aid of the pharynx expression of mCherry introduced as a selection marker together with MosOpn3. The expression of MosOpn3 in ASH neurons was confirmed by the expression of GFP, which was designed to be bicistronically expressed with MosOpn3 in ASH neurons. We performed behavioral experiments (Fig. 1*C*) for a light-induced avoidance of MosOpn3-worms that were fed 11-*cis* retinal–containing *Escherichia coli* (MosOpn3/11-worms). As a result, MosOpn3/11-worms exhibited clear avoidance responses by illumination of white light (Fig. 2*A* upper panels, Movie S1*A*). On the other hand, MosOpn3-worms without a supply of retinal (MosOpn3/NoRet-worms) did not exhibit the light-induced avoidance responses at all (Movie S1*B*), which is consistent with previous observations that the addition of retinal is required for functioning of rhodopsins in *C. elegans* (6, 39). The retinal requirement demonstrated that the light-induced avoidance responses of MosOpn3-worms were not caused by the endogenous light sensor protein, lite-1 (43, 44), but indeed by MosOpn3 provably through Gi/o-mediated signaling. Collectively, the results ensure the validity of our experimental conditions including light intensity for investigating the functionality of heterologously expressed animal opsins in *C. elegans*. Importantly, when MosOpn3-worms were fed all-*trans* retinal (MosOpn3/AT-worms), they also exhibited the light-induced avoidance responses (Fig. 2*A, Lower Panels* and Movie S1*C*) like the case of MosOpn3/11-worms, which can be explained by the unique molecular property of MosOpn3, the pigment formation ability with 13-*cis* retinal thermally generated from all-*trans* form as observed in our previous in vitro experiment (22).

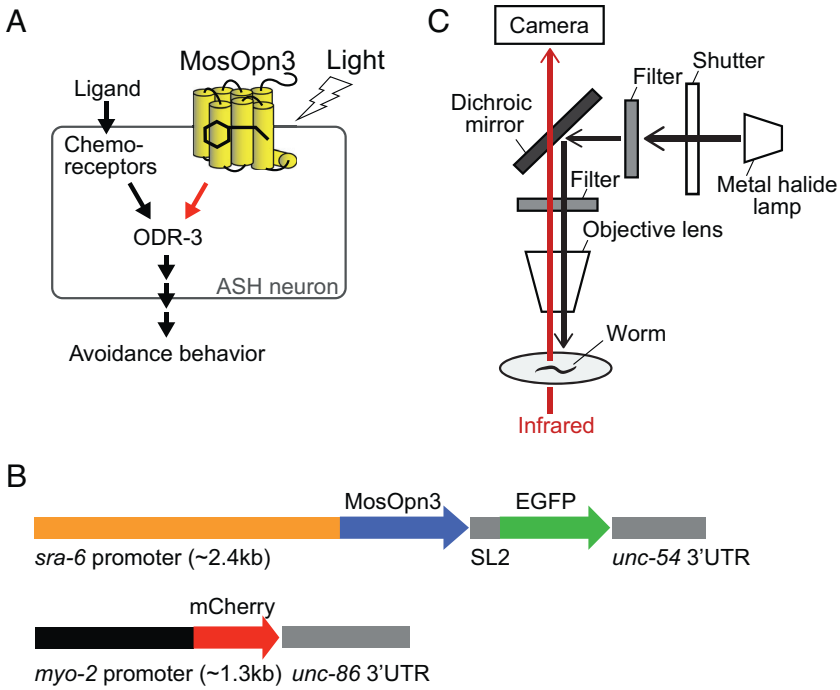

Fig. 1. Examination of the functionality of MosOpn3 in ASH neurons of *C. elegans*. (*A*) The construction for introducing MosOpn3 with EGFP under the *sra-6* promoter. A selection marker mCherry was also introduced under the *myo-2* promoter. (*B*) GPCR signaling in ASH neurons. Activation of ODR-3, a Gi-like protein eventually causes avoidance behavior of *C. elegans*. (*C*) Experimental setup. Worms were continuously monitored with infrared light. Light stimuli were supplied using a dichroic mirror, and the intensities were regulated with ND filters.

Comparison of the Functionality and Efficiency In Vivo between MosOpn3 and BovRh. To evaluate the advantage of MosOpn3 in optical control of GPCR signaling in vivo, we also investigated the light-induced avoidance behaviors of Tg *C. elegans* expressing a bleaching opsin, bovine rhodopsin (BovRh), which activates Gi/o-type G protein (45) like MosOpn3 and does not bind 13-*cis* retinal or all-*trans* retinal unlike MosOpn3. Tg worms established to express BovRh in ASH neurons (BovRh-worms) exhibited the avoidance behavior by white light illumination when they were fed 11-*cis* retinal–containing *E. coli* (Movie S1 *D* and *E*). On the other hand, BovRh-worms did not respond to light when they were fed all-*trans* retinal–containing *E. coli* (Movie S1*F*), which is different from the case of MosOpn3/AT-worms, showing good agreement with molecular properties of respective opsins. We then compared the performances of these two animal opsins in optical control of GPCR signaling in vivo quantitatively. We investigated the relationships between light intensity and light-induced avoidance response probabilities of MosOpn3- and BovRh-worms with various amounts of 11-*cis* retinal to find the necessary amount of 11-*cis* retinal for functioning in ASH neurons to avoid side effects caused by an excess amount of retinal. The light intensity–response probability relationships revealed that MosOpn3-worms exhibited a similar light sensitivity even when the amount of 11-*cis* retinal was reduced to 1/100, and the sensitivity was slightly decreased under 1/1,000 amount of 11-*cis* retinal (*SI Appendix*, Fig. S1*A*). In the case of BovRh-worms, the light sensitivity was also similar even when the amount of 11-*cis* retinal was reduced to 1/100, but the sensitivity was largely decreased under 1/1,000 amount of 11-*cis* retinal (*SI Appendix*, Fig. S1*B*). These results indicate that the 1/100 amount is necessary to induce maximum performance for both opsins in this behavior. We then compared performances of MosOpn3- and BovRh-worms in the presence of the minimum necessary amount of retinal. We found that light sensitivities of MosOpn3/11- and BovRh/11-worms are similar, which suggests a similarity in performance of 11-*cis*–binding MosOpn3 and BovRh in the ASH neurons (Fig. 2 *B* and *E*). On the other hand, in the same amount of all-*trans* retinal, MosOpn3/AT-worms exhibited the avoidance responses by illuminations of 1/10,000~1/1,000 of the maximum intensity (I_0) of light, whereas BovRh/AT-worms did not exhibit any avoidance responses even by illuminations of the maximum intensity of light (Fig. 2 *C* and *F*), demonstrating that the sensitivity of MosOpn3/AT-worms is more than 1,000 times higher than that of BovRh/AT-worms. Remarkably, the sensitivity of MosOpn3/AT-worms is comparable with that of MosOpn3/11-worms (Fig. 2*C*). In addition, when the amounts of 11-*cis* and all-*trans* retinal added to worms were reduced to 10 times lower level (1/1,000 of the standard amount), the sensitivities of MosOpn3-worms in the presence of 11-*cis* and all-*trans* retinal decreased similarly (Fig. 2 *C*, *D*, and *G*). Since the decreases of sensitivity are explained by those of formed photopigment amount in *C. elegans*, the similarities in sensitivity between MosOpn3/11- and MosOpn3/AT-worms under varied retinal amounts suggest that MosOpn3 bound to 11-*cis* retinal and MosOpn3 bound to 13-*cis* retinal, which is thermally generated from all-*trans* retinal, can function with similar efficiency in ASH neurons. These results clearly demonstrated that MosOpn3 performs efficiently in ASH neurons to evoke avoidance responses even in the presence of all-*trans* retinal like microbial rhodopsins.

Engineering MosOpn3 for Light-Dependent Upregulation of Intracellular cAMP and Ca2+ Levels. MosOpn3 forms a photopigment by binding 13-*cis* retinal to activate Gi- and Go-type G proteins in a light-dependent manner (22), which leads to a decrease in cAMP. To expand the scope of optogenetic application of MosOpn3, we engineered MosOpn3 to up-regulate cAMP and Ca^{2+} levels, through Gs- or Gq-type G protein, respectively, by exchanging the cytoplasmic region(s) including the third cytoplasmic loop, the major determinant of G protein selectivity for Class A

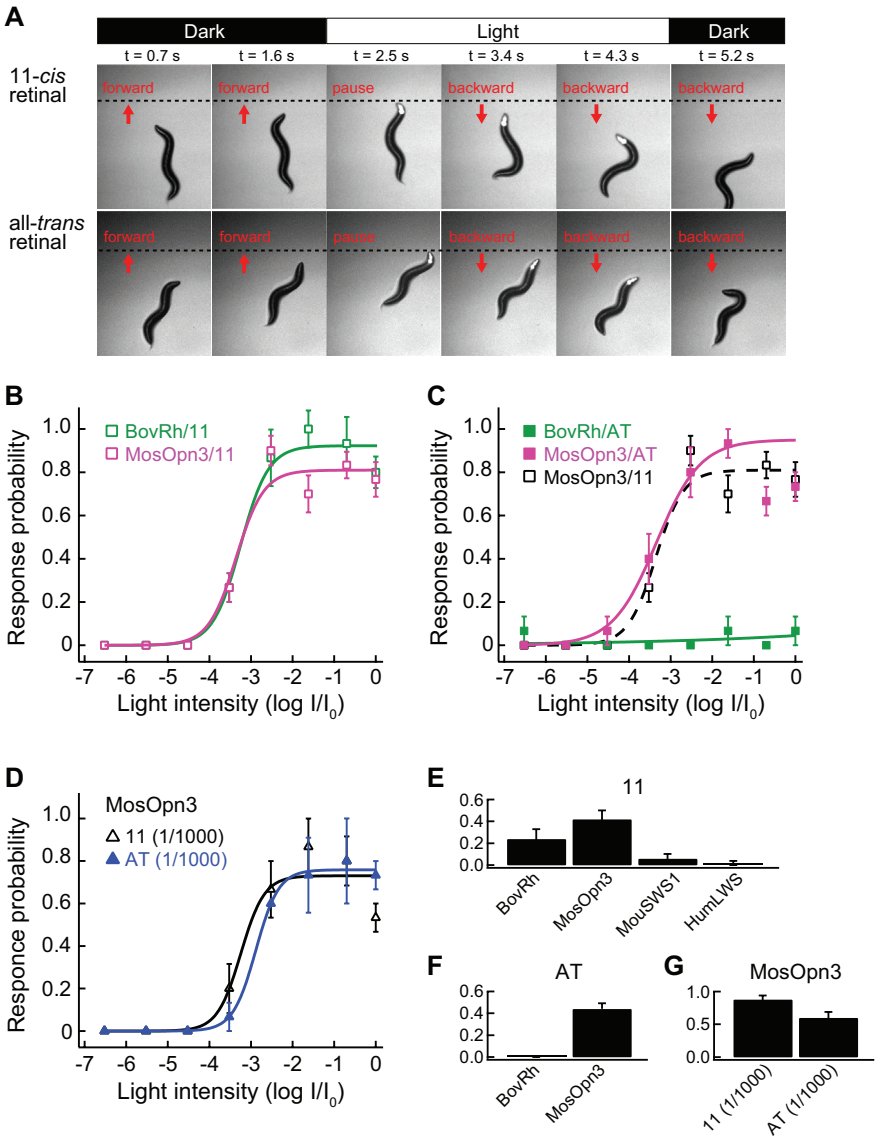

Fig. 2. Functionality of MosOpn3 in ASH neurons of *C. elegans*. (*A*) Snapshot images at 0.7, 1.6, 2.5, 3.4, 4.3, and 5.2 s after recording start, showing light-induced avoidance responses of MosOpn3-expressing Tg worms in the presence of 11-*cis* (*Upper*) and all-*trans* (*Lower*) retinal. The horizontal bar and mCherry signals emitted by the light illumination indicate the timing of white light stimulus. Dotted lines indicate the position of the frontal tip of worms when they stopped moving forward. (*B* and *C*) White light intensity–response probability relationships for MosOpn3-worms (magenta squares and curve) and BovRh-worms (green squares and curve) in the minimum necessary amount (1/100 of the standard amount of retinal) 11-*cis* retinal (*B*, n = 6) and all-*trans* retinal (*C*, n = 3). Both Tg worms exhibited a similar light sensitivity in the case of 11-*cis* retinal, whereas only MosOpn3-worms responded to light in the presence of all-*trans* retinal. The light intensity–response probability relationship for MosOpn3/11-worms is also indicated in (*C*) for a comparison (black open squares and dashed curve), showing a similar performance of MosOpn3/11- and MosOpn3/AT-worms in the light-induced avoidance behavior. (*D*) White light intensity–response probability relationships for MosOpn3/11-worms (black triangles) and MosOpn3/AT-worms (blue triangles) in the presence of 1/1,000 of the standard amount of retinal (n = 3). (*E*–*G*) Response probabilities of Tg worms at critical light intensities for *B* (*E*, $I = 3 \times 10^{-4} I_0$), *C* (*F*, $I = 3 \times 10^{-4} I_0$), and *D* (*G*, $I = 3 \times 10^{-3} I_0$) were evaluated (n = 10). The data for MouSWS1- and HumLWS-worms in the presence of the standard amount of 11-*cis* retinal are also shown. I_0 = ~0.8 mW/mm^2 (*B*–*G*).

GPCRs (45–51). We chose the ß2-adrenergic receptor (ß2AR) and α1-adrenergic receptor (α1AR), which are generally considered to selectively activate Gs- and Gq-type G proteins, respectively, as donor GPCRs. We generated a series of MosOpn3-ß2AR and MosOpn3-α1AR chimeras, in which the cytoplasmic region(s) were replaced with those of ß2AR or α1AR according to previous reports (5, 50), and investigated functional conversion. In the case of MosOpn3-ß2AR chimeras, we measured light-induced increases of the cAMP level in cultured cells expressing each chimera using the GloSensor cAMP assay and revealed that all chimeras induced obvious cAMP increases light dependently in contrast to the cAMP decrease in the wild type (WT) even without addition of retinal (Fig. 3*A*), indicating successful conversion of cAMP regulation from down- to upregulation by MosOpn3 bound to endogenous retinal in the culture medium. Any MosOpn3-ß2AR chimeras exhibited larger cAMP increases upon light absorption than the previously reported MosOpn3 chimera containing the third cytoplasmic loop of jellyfish Gs-coupled opsin (20, 26). Among all, the chimera in which all cytoplasmic regions were replaced with those of ß2AR (MosOpn3-ß2ARiL123C) exhibited the largest cAMP increase, and the chimera containing the second and third cytoplasmic loops, and C-terminal region of ß2AR (MosOpn3-ß2ARiL23C) was comparable. An interesting finding is that introducing the first cytoplasmic loop of ß2AR accelerates the reversion of increased cAMP levels to the basal level, which provides choices of different kinetics of cAMP changes based on the chimera species (Fig. 3*A*).

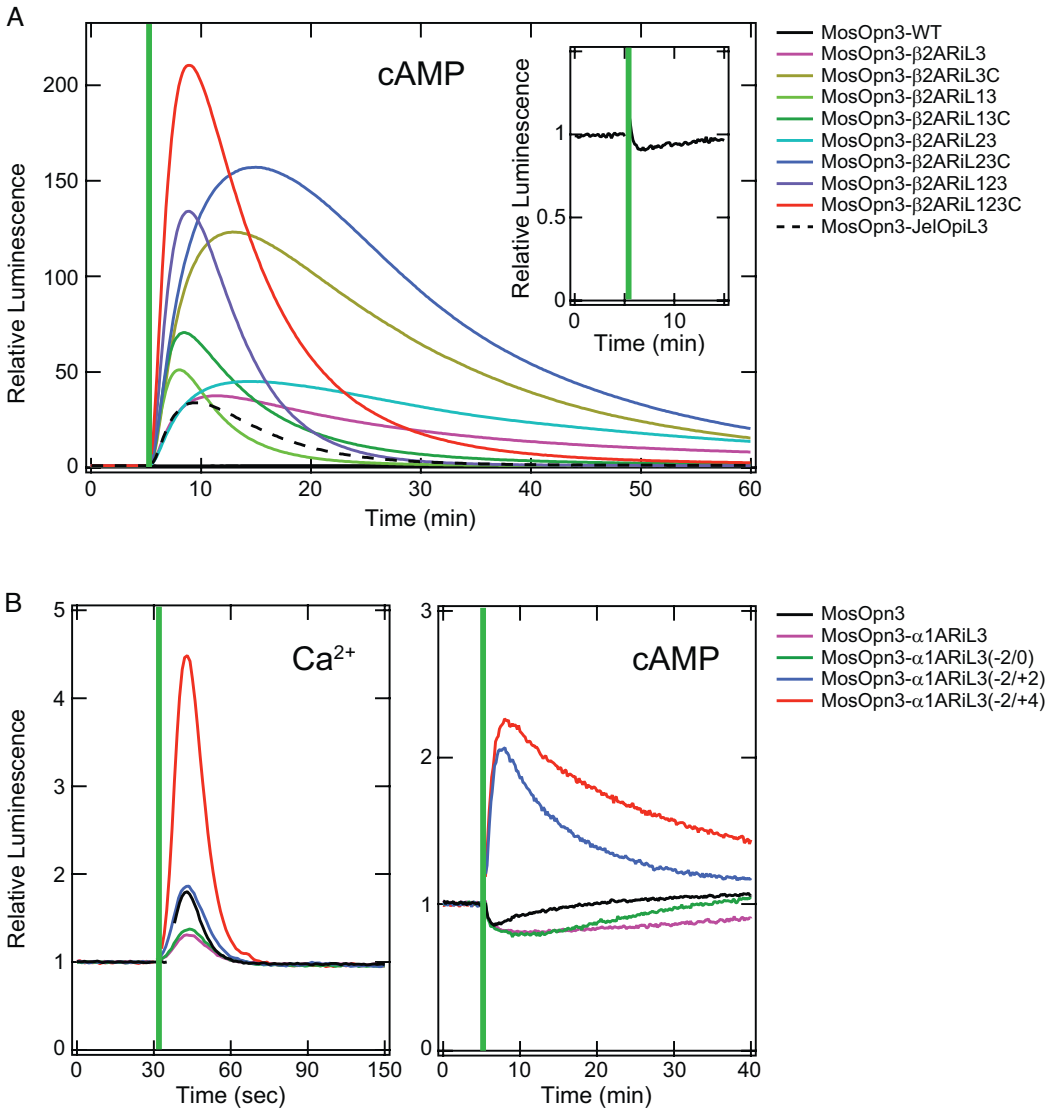

Fig. 3. Engineering MosOpn3-based tools to activate Gs- or Gq-type G protein. (*A*) GloSensor cAMP assay with HEK293 cells expressing various MosOpn3-ß2AR chimeras, showing light-induced increases of intracellular cAMP levels. MosOpn3 chimera containing the third cytoplasmic loop of jellyfish Gs-coupled opsin (MosOpn3-JelOpiL3) is also shown for a comparison. The light-induced cAMP decrease in HEK293 cells expressing MosOpn3 WT is shown in *Inset*. Vertical lines indicate light illumination for 5 s. (*B*) Aequorin Ca^{2+} assay with HEK293 cells expressing MosOpn3-α1ARiL3 chimeras having varied lengths of the third cytoplasmic loop of α1AR, showing light-induced increases of intracellular Ca^{2+} levels (*Left*). Light-induced changes of intracellular cAMP levels of HEK293 cells expressing the MosOpn3-α1AR chimeras are also shown (*Right*). Note that other MosOpn3-α1AR chimeras did not show significant improvement of light-induced Ca^{2+} elevation. Vertical lines indicate light illumination for 1 s (*Left*) and 5 s (*Right*).

Regarding the regulation of Ca^{2+} level, aequorin luminescence-based calcium assay revealed that MosOpn3 WT originally exhibited a light-induced Ca^{2+} increase in cultured cells (Fig. 3*B*), although it also induced a decrease in the cAMP level as described previously (22) (Fig. 3 *A* and *B*). Then, we evaluated specific regulation of Ca^{2+} by MosOpn3-α1AR chimeras in cultured cells expressing each chimera. Contrary to the case of MosOpn3-ß2AR chimeras, only the MosOpn3-α1AR chimera having the third cytoplasmic loop of α1AR (MosOpn3-α1ARiL3) exhibited a light-induced Ca^{2+} increase under the condition without 11-*cis* retinal addition, although the Ca^{2+} increase by the chimera is less than that that by the WT, and the chimera still exhibited a cAMP decrease (Fig. 3*B*). To improve the specificity of the MosOpn3-α1ARiL3 for a Ca^{2+} increase, we further engineered the chimera by fine-tuning of the third cytoplasmic loop to be exchanged by shifting the donor/acceptor boundaries by two or four amino acids. In all possible combinations, we found that chimeras generated by reduction of two amino acids at the N-terminal and addition of four amino acids at the C-terminal of the third cytoplasmic loop of α1AR (MosOpn3-α1ARiL3(−2/+4)) exhibited the highest functionality in light-induced Ca^{2+} elevation, which is ~2.5-fold higher than the case of WT without a cAMP decrease. The light-induced cAMP increases observed in the case of MosOpn3-α1ARiL3(−2/+4) and MosOpn3-α1ARiL3(−2/+2) were presumably caused by Ca^{2+} elevation (52–54). These results suggest the practical strategy for creating on-demand optogenetic tools based on MosOpn3 for controlling intracellular cAMP and Ca^{2+} levels probably through optimizing G protein signaling preference.

Parapinopsin for Color-Dependent Control of GPCR Signaling. In cases of visible light–sensitive bistable opsins including MosOpn3, the dark (inactive) and photoproduct (active) states have largely overlapped absorption spectra in the visible light region. On the contrary, in the case of parapinopsin, the absorption spectra of the UV-sensitive inactive state and visible light–sensitive active state are distinct from each other, enabling to illuminate only

the active state with visible light, which leads to complete regeneration of the inactive state. To evaluate the contribution of the photoregeneration ability in optical control of GPCR signaling in vivo, we focused on another *C. elegans* behavior, coordinated movement regulated by acetylcholine. Using the *unc-17* promoter, we introduced LamPP into cholinergic motor neurons, in which activation of Go-mediated signal transduction down-regulates acetylcholine releases to lead uncoordinated movement including coiling of *C. elegans* (55, 56) (Fig. 4 *A* and *B*). Tg worms expressing LamPP in cholinergic motor neurons (LamPP-worms) were obtained with the same procedure as that for MosOpn3-worms. When we illuminated LamPP-wormsfed 11-*cis* retinal–containing *E. coli* with violet light, the Tg worms stopped moving and coiled as expected, and upon subsequent green light illumination, the Tg worms restarted coordinated movement (Fig. 4 *C* and *D* and Movie S2). The violet light–induced coiling of LamPP-worms sustained for 30 min after the turnoff of light, and subsequent green light illumination restored the movement (Fig. 4*E*). The

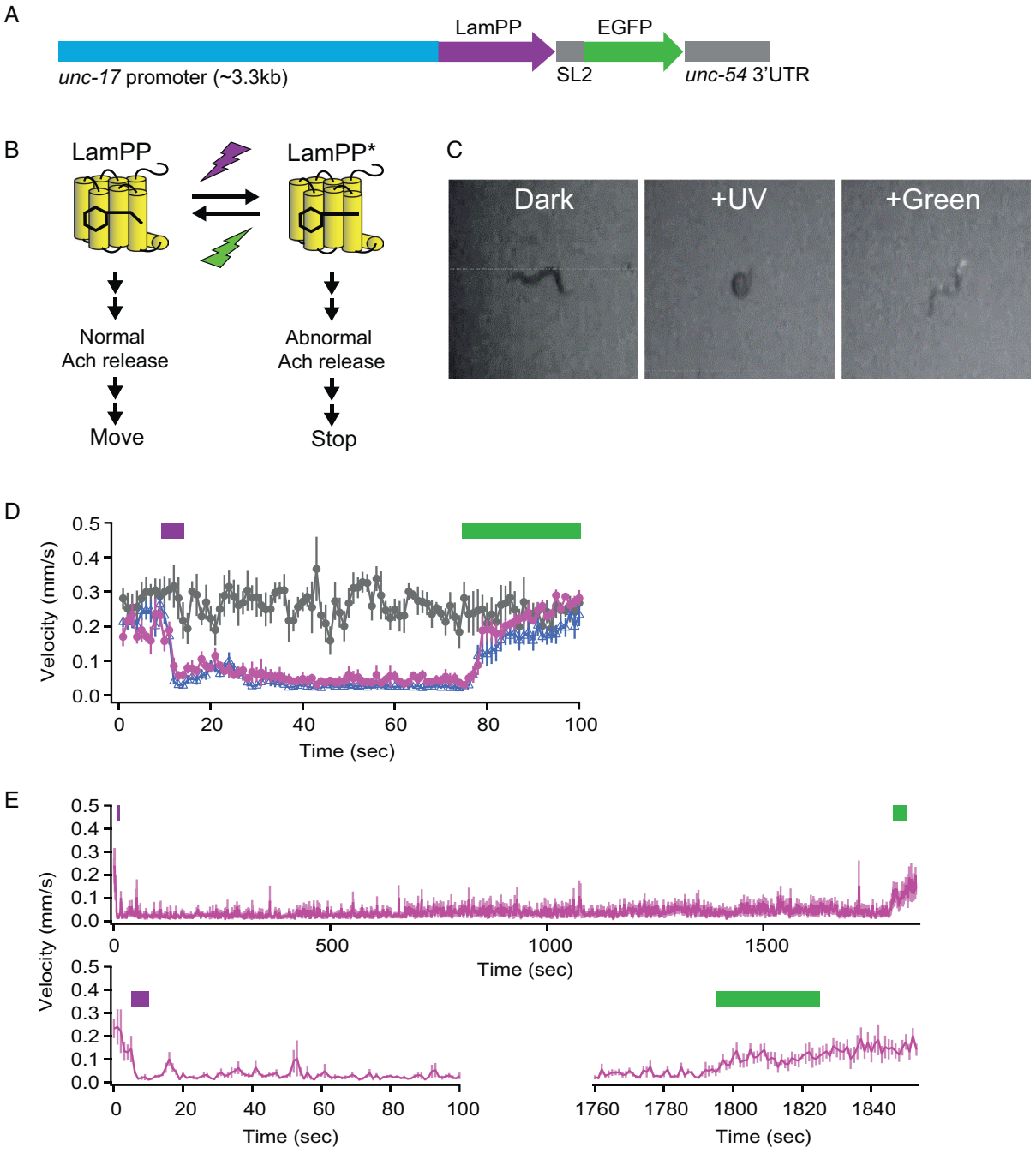

Fig. 4. Color-dependent control of Tg *C. elegans* expressing LamPP in cholinergic motor neurons. (*A*) The construction for introducing LamPP with EGFP under the *unc-17* promoter. (*B*) A schematic drawing of the relationship between status of LamPP and *C. elegans* behavior caused by violet and green light illumination. LamPP* indicates the active state of LamPP. (*C*) Snapshot images of the behavior of *C. elegans* expressing LamPP in cholinergic neurons in the dark, after violet illumination, and subsequent green light illumination, showing moving forward, coiling, and restart moving, respectively (Movie S2). (*D*) Quantitative evaluation of violet light–induced coiling and subsequent green light–induced recovery of LamPP-worms (n = 5). LamPP-worms fed *E. coli* without retinal (gray circles), with 11-*cis* retinal (magenta circles) in the dark, and with all-*trans* retinal (blue circles) under the red light were illuminated with violet light for 5 s (violet line), kept in the dark for 1 min, and illuminated with green light for 30 s (green line). (*E*) Violet light–induced coiling of LamPP-worms fed 11-*cis* retinal sustained for 30 min after turnoff of the violet light. All worms exhibited immobility and/or coiling for 30 min. Upon green illumination, all worms restarted moving.

behavioral switching between coiling and moving upon violet and green light stimuli occurred repeatedly (Movie S2), demonstrating color-dependent control of the *C. elegans* behavior using LamPP. In other words, the result suggested that introducing LamPP into cells containing Gi/o-mediated signaling could render physiologies color dependency. Furthermore, LamPP-wormsfed all-*trans* retinal under the red light (600 nm) exhibited violet light–induced stop and green light–induced recovery like the case of LamPP-wormsfed 11-*cis* retinal (Fig. 4*D*). Since retinal hardly absorbs red light, the phenomena can be explained by the complete photoregeneration ability of LamPP; LamPP bound all-*trans* retinal to form the active state (LamPP* in Fig. 4*B*) directly, and the active state completely converted to the 11-*cis* retinal–binding inactive state by red light absorption.

Again, we engineered LamPP, which originally activates Gi/o-type G protein, to activate Gs-type G protein to up- and down-regulate intracellular cAMP levels with violet and visible light absorption, respectively, which is in the opposite direction caused by the WT. We generated a series of LamPP chimeras, in which the cytoplasmic region(s), including the third cytoplasmic loop, was replaced with those of ß2-adrenergic receptor as in the case of engineering Gs-coupled MosOpn3. Light-induced changes of the cAMP level in cultured cells expressing each chimera were measured using the GloSensor cAMP assay. We found that only the cells expressing the chimera containing the third cytoplasmic loop alone (LamPP-ß2ARiL3) exhibited a significant violet light–induced increase in the cAMP level, which in turn decreased to the basal level by subsequent green light illumination (Fig. 5*A*). The color-dependent upregulations and downregulations of cAMP levels occurred repeatedly. Notably, the cAMP increases induced by activation of the chimera were composed of two phases; upon violet light illumination, cAMP levels rapidly increased to a higher level and immediately decreased to a lower level (acute phase), and the lower level sustained for more than 1 h until green light illumination (chronic phase). Interestingly, when LamPP-ß2ARiL3–expressing cells were illuminated with blue light, the cAMP level was set at a level between levels caused by violet and green light illumination (Fig. 5*B*). Furthermore, the cAMP levels caused by blue light illumination were almost constant regardless of the levels just before illumination. The color dependency of the sustained cAMP level could be explained in part by color-dependent photoequilibrium of the inactive and active states of LamPP (17, 35). We also tested the performance of an additional LamPP chimera containing the third cytoplasmic loop of the jellyfish Gs-coupled opsin, LamPP-JelOpiL3. The LamPP-JelOpiL3 exhibited much higher amplitude of violet light–induced cAMP increases compared with LamPP-ß2ARiL3, whereas the increased cAMP level gradually decreased (*SI Appendix*, Fig. S2), unlike the case of LamPP-ß2ARiL3. The increase and decrease in the cAMP level by violet light and green light illumination also occurred repeatedly for LamPP-JelOpiL3. Collectively, these Gs-coupled LamPPs enable to control Gs-mediated signal transduction in a color-dependent manner, showing successful expansion of LamPP as tools for color-dependent control of GPCR signaling.

Discussion

In this study, we demonstrated high performances of two bistable opsins, MosOpn3 and LamPP, in controlling GPCR signalings in vivo. Tg worms expressing MosOpn3 in ASH neurons exhibited light-induced avoidance behaviors in the presence of 11-*cis* retinal and all-*trans* retinal with a similar sensitivity, which is

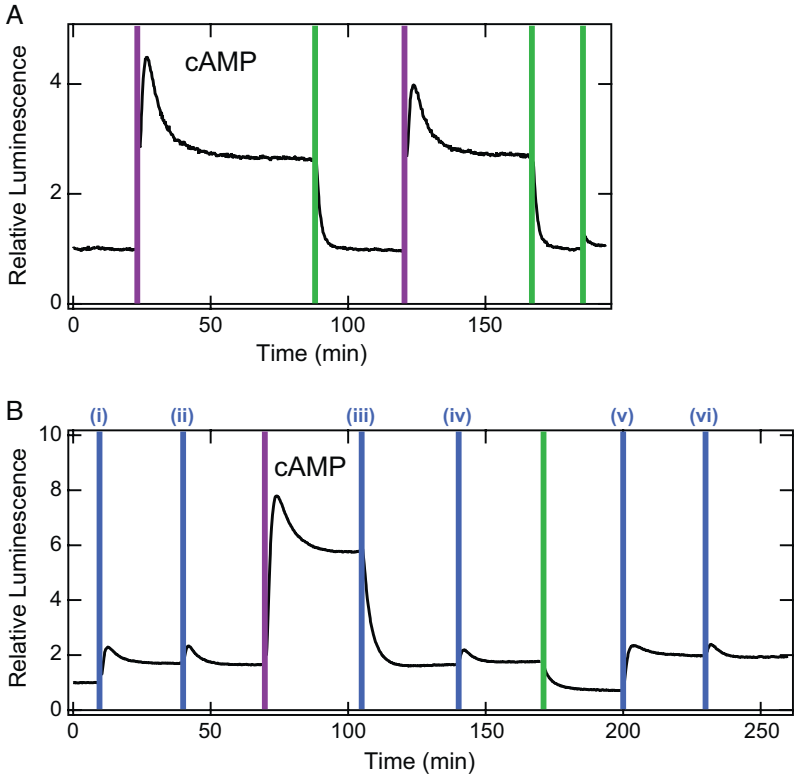

Fig. 5. Color-dependent control of cAMP level by LamPP-ß2ARiL3 through the activation of Gs-type G protein. (*A*) Violet light illumination increased intracellular cAMP levels in HEK293 cells expressing LamPP-ß2ARiL3, and subsequent green light illumination decreased the cAMP level to the basal level, which occurred repeatedly. (*B*) Blue light illumination generated a particular cAMP level. The cAMP levels generated by i) the first illumination, ii) the subsequent illumination, iii) the illumination after violet light illumination, iv) the subsequent illumination, v) the illumination after green light illumination, and vi) the subsequent illumination of blue light were almost constant, showing color-dependent cAMP clamping. Vertical lines indicate light illumination for 5 s.

comparable with the case of Tg worms expressing bovine rhodopsin (BovRh) in the presence of 11-*cis* retinal (Figs. 1 and 2). We also tested the performance of Tg worms expressing mouse SWS1 opsin (MouSWS1) and human LWS opsin (HumLWS), which are known opsin-based tools having Go activation ability (57), in the presence of 11-*cis* retinal, but the performances are less than that of BovRh (Fig. 2*E*). On the other hand, BovRh-worms did not exhibit light-induced avoidance behaviors in the presence of all-*trans* retinal as shown in the previous report examining the functionality of BovRh in other type of neurons of *C. elegans*, in which 9-*cis* retinal addition induced light-dependent neural responses, but all-*trans* retinal addition did not (6). Since all-*trans* retinal is basically present in every tissue, the performance of MosOpn3 in the presence of all-*trans* retinal comparable with that of BovRh under the 11-*cis* retinal suggests that MosOpn3 has a crucial advantage in optical control of GPCR signaling in vivo. It is widely accepted that microbial rhodopsins such as ChR2 are powerful tools for use in optogenetics, especially in optical control of neural activities (58–61). One of the reasons for the popularity is that microbial rhodopsins form photosensitive pigments by binding all-*trans* retinal to function in every tissue, and the 11-*cis* retinal requirement of bleaching opsins is the main reason for unpopularity of animal opsins. In terms of this point, the current study demonstrated that the availability of MosOpn3 could be equivalent to that of microbial rhodopsins. Moreover, the sensitivity of the avoidance response light dependently induced by MosOpn3 in ASH neurons was revealed to be ~0.0002 mW/mm^2 (white light) in the presence of all-*trans* retinal (Fig. 2*C*), which is ~7,000 times higher than that induced by ChR2 in ASH neurons (~1.48 mW/mm^2, blue light) reported in the previous study (62). In fact, we generated Tg worms expressing ChR2 in ASH neurons and tested light-induced avoidance behaviors with the same protocol as in cases of MosOpn3 and BovRh, but no reproducible avoidance response was observed by illuminating with ~0.8 mW/mm^2 of white light, the highest light intensity of our light source. These data demonstrated that MosOpn3 could function as a light-sensitive switch to provide much higher photosensitivity to any tissue with much lower light–induced toxicity and/or temperature increase compared with the case of ChR2. There was a potential concern that the basal activity of 13-*cis* retinal–bearing MosOpn3 pigment might affect cellular conditions intrinsically in vivo because the activity of G protein by the 13-*cis* retinal–bearing pigment in the dark was higher than that of the 11-*cis* retinal–bearing pigment (22). However, MosOpn3-wormsfed all-*trans* retinal–containing *E. coli*, in which 13-*cis* retinal–bearing MosOpn3 pigments formed, normally behaved in the dark (Fig. 2, Movie S1 *C*). The data suggest that intracellular conditions in ASH neurons were somehow maintained to be normal, even with the partial G protein activation by 13-*cis* retinal–bearing MosOpn3 pigment. Then, we established ß2AR (Gs-coupled receptor) and α1AR (Gq-coupled receptor) versions of MosOpn3 by replacing the cytoplasmic region(s) with those of ß2AR and α1AR, respectively, to expand the applicability of MosOpn3 (Fig. 3). Analysis of a series of MosOpn3 chimeras revealed that fine-tuning of replaced regions improves the G protein activation efficiency and specificity (α1ARiL3) and alters the kinetics of chimeras (ß2AR), which could be a guide for making various MosOpn3 chimeras with other GPCRs of interest for appropriate purposes.

We also demonstrated color-dependent control of GPCR signaling by LamPP to lead behavioral switching between coiled and moving of *C. elegans* upon violet and green light stimuli, respectively (Fig. 4 *D* and *E*). The switching is consistent with the molecular behavior of LamPP by UV and visible light absorption (17), which suggests that the photoregeneration ability of LamPP contributes to the mode change of animal behaviors. Interestingly, we recently reported that in the zebrafish pineal photoreceptor cells, the parapinopsin alone generates color opponency; UV and orange lights induce hyperpolarization and depolarization, respectively, based on the photoequilibrium levels between the inactive and active states of the parapinopsin (35). The idea was also supported by the current results by heterologous expressions of LamPP in *C. elegans* neurons, showing that introducing LamPP is sufficient for color-dependent behavioral switching. Furthermore, we demonstrated that LamPP-wormsfed all-*trans* retinal under the red light (600 nm) responded to light stimuli (Fig. 4*E*), indicating that LamPP could function as a light-sensitive switch in the presence of all-*trans* retinal, in other words, in every tissue with red light preillumination. Accordingly, with red light, LamPP is optogenetically available in every tissue, which is practically equivalent to MosOpn3 as well as microbial rhodopsins.

The color-dependent control of Gi/o-type G protein by the wild-type LamPP has also been expanded to that of Gs-type G protein by LamPP-ß2ARiL3 and LamPP-JelOpiL3, which enables color-dependent control of intracellular cAMP levels in the reverse direction to the reactions by the WT (Fig. 5). Interestingly, LamPP-ß2ARiL3 showed molecular properties for not only color-dependent switch on and switch off of GPCR signaling but also color-dependent and context-independent maintenance of the intracellular cAMP level (Fig. 5). The results indicate that LamPP-ß2ARiL3 achieves clamping intracellular cAMP levels depending on color of light. We also emphasize that the cAMP levels were maintained in the dark after a light flash, depending on its color, suggesting an alternative strategy for "light" regulation of the cAMP level. On the other hand, the "cAMP clamping" was not achieved in the case of LamPP-JelOpiL3 (*SI Appendix*, Fig. S2). The clamped cAMP level could relate to shut off manners of the active state of LamPP-ß2ARiL3 based on unknown effects of the third cytoplasmic loop of ß2AR including phosphorylation and/or arrestin binding, which provides a new insight into prolongation of GPCR signalings.

In this study, the availability of two bistable animal opsins has shown to be equivalent to that of microbial rhodopsins including ChR2 in terms of retinal requirement, which would accelerate research by optical control of GPCR signaling. In controlling GPCR signaling, chemical control, namely chemogenetics using chemoreceptors such as designer receptor exclusively activated by designer drugs (DREADD), has been widely used (63–65), which is in contrast to the situation of optogenetics with animal opsins, mainly bleaching opsins. The low popularity of optical control of GPCR signaling was mainly due to the absence of effective and robust tools, but the situation has been recently changing with bistable opsins, especially MosOpn3 and LamPP (28, 36–38), and advantages of them and their derivatives were systematically demonstrated based on their molecular properties in this paper. The main advantage of chemogenetics is that stimuli (chemicals) can be reliably delivered deep inside the body. On the other hand, temporally precise control of GPCR signaling in vivo is basically unachievable by chemogenetics but achievable by optogenetics. In particular, temporally precise termination of G protein signaling as demonstrated by LamPP (Figs. 4 and 5) is a significant advantage of optogenetics, which enables controlling durations, intervals, and numbers of the stimuli. Together with chemical control, the optical control with bistable animal opsins would greatly facilitate comprehensive and deeper understating of GPCR-based physiologies as well as GPCR signaling itself.

Materials and Methods

Generating Tg *C. elegans*. Based on the information from WormBase (66), the 2.4-kbp promoter sequence of *sra*-6 (42) was obtained from the *C. elegans* genomic DNA by PCR. The 3.3-kbp promoter sequence of *unc*-17 was a generous gift from Prof. Robert Lucas (56). The vector backbone containing SL1 and GFP was obtained by digestion of the plasmid [pEM1 = flp-21::LoxPStopLoxP::npr-1 SL2 GFP] (Addgene plasmid # 24033) (67) with NotI and KpnI. The *sra*-6 promoter linked with MosOpn3 (AB753162), bovine rhodopsin (AB062417), mouse SWS1 opsin (U49720), and human LWS opsin (NM_020061) cDNA or the *unc-17* promoter linked with LamPP cDNA was introduced into the vector. Each plasmid was coinjected into the wild-type *C. elegans* strain N2 obtained from the Caenorhabditis Genetics Center with *pmyo-2::mCherry* as a selection marker. The wild and Tg strains (*psra-6::MosOpn3::GFP, psra-6::BovRh::GFP, psra-6::MouSWS1::GFP, psra-6::HumL-WS::GFP*, and *punc-17::LamPP::GFP*) were cultured according to standard methods (68). The plasmids and strains are available on request.

Behavioral Experiments. Adult worms were used for behavioral experiments. Tg worms were fed *E. coli* strain OP50, which are mixed with or without certain amounts of retinal at 24 h before experiments. The standard concentration of 11-*cis* retinal or all-*trans* retinal in OP50 for our experiment was 0.38 mM or 0.67 mM, respectively, and diluted to 1/100 to 1/10,000. Worms were monitored under infrared light illumination. White lights ($I_0 = \sim 0.8$ mW/mm^2) supplied by a 200-W metal-halide lamp (PhotoFluor II, 89 North) with or without ND filter(s) were applied as light stimuli for MosOpn3-worms. Narrow-band violet (410 nm) and green (510 nm) LED lights were applied as light stimuli for LamPP. Red (600 nm) LED light was used as a background light, while LamPP-worms were fed all-*trans* retinal. Avoidance response probabilities were calculated by the ratio or the number of responded worms to five worms examined.

Generation of Chimeric Mutants of Opsins. Chimeric mutants of MosOpn3 and LamPP were generated by replacing cytoplasmic regions of hamster ß2-adrenergic receptor (ß2AR) and human α1-adrenergic receptor (α1AR) by combining DNA fragments of each region with PCR. The cytoplasmic regions were determined according to previous reports (5, 50) and applied to MosOpn3 and LamPP based on the alignment including bovine rhodopsin. We deposited a set of plasmids for the chimeric mutants in Addgene.

Bioluminescent Reporter Assays for Ca^{2+} and cAMP. The intracellular cAMP and Ca^{2+} levels in opsin-expressing HEK293S cells were measured using the GloSensor cAMP assay and the aequorin assay, respectively, as described previously (22, 26, 69, 70). The pGloSensor-22F cAMP plasmid (Promega) was used for the GloSensor cAMP assay. The wild-type aequorin obtained by introducing two reverse mutations into the plasmid [pcDNA3.1+/mit-2mutAEQ] (Addgene #45539) (71) was used for the aequorin assay. A broadband green LED light and narrow-band violet (410 nm) and blue (430 nm) LED lights were applied for 5 s in the GloSensor cAMP assay and for 1 s in the aequorin assay as light stimuli.

Data, Materials, Software Availability. All study data are included in the article and/or *SI Appendix*. Some study data available (The plasmids and strains are available on request).

ACKNOWLEDGMENTS. We thank Robert J. Lucas (The University of Manchester) for providing the *unc-17* promoter and his helpful comments on this manuscript. We also thank Takahiro Yamashita (Kyoto University) for providing the mouse SWS1 opsin and human LWS opsin clones. This work was supported by the JSPS KAKENHI grant numbers JP18H02482, JP20K21433, and JP21H00435 (M.K.), JP15H05777 and JP20K21434 (A.T.), Japan Science and Technology Agency (JST) Precursory Research for Embryonic Science and Technology (PRESTO) grant JPMJPR13A2 (M.K.), and JST Core Research for Evolutional Science and Technology (CREST) grant JPMJCR1753 (A.T.).

Author affiliations: [a]Department of Biology, Graduate School of Science, Osaka Metropolitan University, Sumiyoshi-ku, Osaka 558-8585, Japan; [b]The OMU Advanced Research Institute for Natural Science and Technology, Osaka Metropolitan University, Sumiyoshi-ku, Osaka 558-8585, Japan; [c]Department of Biology and Geosciences, Graduate School of Science, Osaka City University, Sumiyoshi-ku, Osaka 558-8585, Japan; and [d]Department of Nutrition, Graduate School of Human Life and Ecology, Osaka Metropolitan University, Sumiyoshi-ku, Osaka Osaka 558-8585, Japan

1. J. Bockaert, J. P. Pin, Molecular tinkering of G protein-coupled receptors: An evolutionary success. *EMBO J.* **18**, 1723–1729 (1999).
2. K. L. Pierce, R. T. Premont, R. J. Lefkowitz, Seven-transmembrane receptors. *Nat. Rev. Mol. Cell Biol.* **3**, 639–650 (2002).
3. M. C. Lagerstrom, H. B. Schioth, Structural diversity of G protein-coupled receptors and significance for drug discovery. *Nat. Rev. Drug. Discov.* **7**, 339–357 (2008).
4. M. Koyanagi, A. Terakita, Diversity of animal opsin-based pigments and their optogenetic potential. *Biochim. Biophys. Acta* **1837**, 710–716 (2014).
5. R. D. Airan, K. R. Thompson, L. E. Fenno, H. Bernstein, K. Deisseroth, Temporally precise *in vivo* control of intracellular signalling. *Nature* **458**, 1025–1029 (2009).
6. P. Cao *et al.*, Light-sensitive coupling of rhodopsin and melanopsin to G(i/o) and G(q) signal transduction in *Caenorhabditis elegans*. *FASEB J.* **26**, 480–491 (2012).
7. W. K. Karunarathne, L. Giri, V. Kalyanaraman, N. Gautam, Optically triggering spatiotemporally confined GPCR activity in a cell and programming neurite initiation and extension. *Proc. Natl. Acad. Sci. U.S.A.* **110**, E1565–E1574 (2013).
8. M. Koyanagi *et al.*, Optogenetic potentials of diverse animal opsins: Parapinopsin, peropsin, LWS bistable opsin. *Adv. Exp. Med. Biol.* **1293**, 141–151 (2021).
9. H. Tsukamoto, A. Terakita, Diversity and functional properties of bistable pigments. *Photochem. Photobiol. Sci.* **9**, 1435–1443 (2010).
10. A. Terakita *et al.*, Expression and comparative characterization of Gq-coupled invertebrate visual pigments and melanopsin. *J. Neurochem.* **105**, 883–890 (2008).
11. T. Nagata *et al.*, Depth perception from image defocus in a jumping spider. *Science* **335**, 469–471 (2012).
12. T. Nagata *et al.*, The counterion-retinylidene Schiff base interaction of an invertebrate rhodopsin rearranges upon light activation. *Commun. Biol.* **2**, 180 (2019).
13. T. Saito *et al.*, Spectral tuning mediated by helix III in butterfly long wavelength-sensitive visual opsins revealed by heterologous action spectroscopy. *Zoological Lett.* **5**, 35 (2019).
14. H. Ye, M. Daoud-El Baba, R. W. Peng, M. Fussenegger, A synthetic optogenetic transcription device enhances blood-glucose homeostasis in mice. *Science* **332**, 1565–1568 (2011).
15. T. Tsunematsu, K. F. Tanaka, A. Yamanaka, A. Koizumi, Ectopic expression of melanopsin in orexin/hypocretin neurons enables control of wakefulness of mice *in vivo* by blue light. *Neurosci. Res.* **75**, 23–28 (2013).
16. M. van Wyk, J. Pielecka-Fortuna, S. Lowel, S. Kleinlogel, Restoring the ON switch in blind retinas: Opto-mGluR6, a next-generation, cell-tailored optogenetic tool. *PLoS Biol.* **13**, e1002143 (2015).
17. M. Koyanagi *et al.*, Bistable UV pigment in the lamprey pineal. *Proc. Natl. Acad. Sci. U.S.A.* **101**, 6687–6691 (2004).
18. H. Tsukamoto, A. Terakita, Y. Shichida, A rhodopsin exhibiting binding ability to agonist all-*trans*-retinal. *Proc. Natl. Acad. Sci. U.S.A.* **102**, 6303–6308 (2005).
19. M. Koyanagi, K. Kubokawa, H. Tsukamoto, Y. Shichida, A. Terakita, Cephalochordate melanopsin: Evolutionary linkage between invertebrate visual cells and vertebrate photosensitive retinal ganglion cells. *Curr. Biol.* **15**, 1065–1069 (2005).
20. M. Koyanagi *et al.*, Jellyfish vision starts with cAMP signaling mediated by opsin-G(s) cascade. *Proc. Natl. Acad. Sci. U.S.A.* **105**, 15576–15580 (2008).
21. T. Nagata, M. Koyanagi, H. Tsukamoto, A. Terakita, Identification and characterization of a protostome homologue of peropsin from a jumping spider. *J. Comp. Physiol. A* **196**, 51–59 (2010).
22. M. Koyanagi, E. Takada, T. Nagata, H. Tsukamoto, A. Terakita, Homologs of vertebrate Opn3 potentially serve as a light sensor in nonphotoreceptive tissue. *Proc. Natl. Acad. Sci. U.S.A.* **110**, 4998–5003 (2013).
23. M. Koyanagi *et al.*, Diversification of non-visual photopigment parapinopsin in spectral sensitivity for diverse pineal functions. *Bmc Biol.* **13**, 73 (2015).
24. X. J. He, M. R. Banghart, It's lights out for presynaptic terminals. *Neuron* **109**, 1755–1757 (2021).
25. S. Blackshaw, S. H. Snyder, Encephalopsin: A novel mammalian extraretinal opsin discretely localized in the brain. *J. Neurosci.* **19**, 3681–3690 (1999).
26. T. Sugihara, T. Nagata, B. Mason, M. Koyanagi, A. Terakita, Absorption characteristics of vertebrate non-visual opsin, Opn3. *PLoS One* **11**, e0161215 (2016).
27. A. Terakita, T. Nagata, Functional properties of opsins and their contribution to light-sensing physiology. *Zoolog. Sci.* **31**, 653–659 (2014).
28. M. Mahn *et al.*, Efficient optogenetic silencing of neurotransmitter release with a mosquito rhodopsin. *Neuron* **109**, 1621–1635.e8 (2021).
29. S. Blackshaw, S. H. Snyder, Parapinopsin, a novel catfish opsin localized to the parapineal organ, defines a new gene family. *J. Neurosci.* **17**, 8083–8092 (1997).
30. S. Wada, E. Kawano-Yamashita, M. Koyanagi, A. Terakita, Expression of UV-sensitive parapinopsin in the iguana parietal eyes and its implication in UV-sensitivity in vertebrate pineal-related organs. *PLoS one* **7**, e39003 (2012).
31. M. Koyanagi, E. Kawano-Yamashita, S. Wada, A. Terakita, Vertebrate bistable pigment parapinopsin: Implications for emergence of visual signaling and neofunctionalization of non-visual pigment. *Front. Ecol. Evol.* **5**, 23 (2017).
32. A. Terakita *et al.*, Counterion displacement in the molecular evolution of the rhodopsin family. *Nat. Struct. Mol. Biol.* **11**, 284–289 (2004).
33. E. Kawano-Yamashita *et al.*, Activation of transducin by bistable pigment parapinopsin in the pineal organ of lower vertebrates. *PLoS One* **10**, (2015).
34. S. Wada *et al.*, Insights into the evolutionary origin of the pineal color discrimination mechanism from the river lamprey. *Bmc Biol.* **19**, 188 (2021).
35. S. Wada *et al.*, Color opponency with a single kind of bistable opsin in the zebrafish pineal organ. *Proc. Natl. Acad. Sci. U.S.A.* **115**, 11310–11315 (2018).
36. D. Eickelbeck *et al.*, Lamprey parapinopsin ("UVLamP"): A bistable UV-sensitive optogenetic switch for ultrafast control of GPCR pathways. *Chembiochem* **21**, 612–617 (2020).
37. J. Rodgers *et al.*, Using a bistable animal opsin for switchable and scalable optogenetic inhibition of neurons. *EMBO Rep.* **22**, e51866 (2021).
38. B. A. Copits *et al.*, A photoswitchable GPCR-based opsin for presynaptic inhibition. *Neuron* **109**, 1791–1809.e11 (2021).

39. G. Nagel *et al.*, Light activation of channelrhodopsin-2 in excitable cells of *Caenorhabditis elegans* triggers rapid behavioral responses. *Curr. Biol.* **15**, 2279–2284 (2005).
40. K. Roayaie, J. G. Crump, A. Sagasti, C. I. Bargmann, The G alpha protein ODR-3 mediates olfactory and nociceptive function and controls cilium morphogenesis in *C. elegans* olfactory neurons. *Neuron* **20**, 55–67 (1998).
41. M. A. Hilliard, C. Bergamasco, S. Arbucci, R. H. Plasterk, P. Bazzicalupo, Worms taste bitter: ASH neurons, QUI-1, GPA-3 and ODR-3 mediate quinine avoidance in *Caenorhabditis elegans*. *EMBO J.* **23**, 1101–1111 (2004).
42. S. Hori, S. Oda, Y. Suehiro, Y. Iino, S. Mitani, OFF-responses of interneurons optimize avoidance behaviors depending on stimulus strength via electrical synapses. *PLoS Genet.* **14**, e1007477 (2018).
43. S. L. Edwards *et al.*, A novel molecular solution for ultraviolet light detection in *Caenorhabditis elegans*. *PLoS Biol.* **6**, e198 (2008).
44. J. Gong *et al.*, The *C. elegans* Taste receptor homolog LITE-1 is a photoreceptor. *Cell* **167**, 1252–1263.e10 (2016).
45. A. Terakita, T. Yamashita, N. Nimbari, D. Kojima, Y. Shichida, Functional interaction between bovine rhodopsin and G protein transducin. *J. Biol. Chem.* **277**, 40–46 (2002).
46. J. Liu, B. R. Conklin, N. Blin, J. Yun, J. Wess, Identification of a receptor/G-protein contact site critical for signaling specificity and G-protein activation. *Proc. Natl. Acad. Sci. U.S.A.* **92**, 11642–11646 (1995).
47. J. Wess, G-protein-coupled receptors: Molecular mechanisms involved in receptor activation and selectivity of G-protein recognition. *FASEB J.* **11**, 346–354 (1997).
48. M. G. Eason, S. B. Liggett, Chimeric mutagenesis of putative G-protein coupling domains of the alpha2A-adrenergic receptor. Localization of two redundant and fully competent gi coupling domains. *J. Biol. Chem.* **271**, 12826–12832 (1996).
49. T. Yamashita, A. Terakita, Y. Shichida, Distinct roles of the second and third cytoplasmic loops of bovine rhodopsin in G protein activation. *J. Biol. Chem.* **275**, 34272–34279 (2000).
50. J. M. Kim *et al.*, Light-driven activation of beta 2-adrenergic receptor signaling by a chimeric rhodopsin containing the beta 2-adrenergic receptor cytoplasmic loops. *Biochemistry* **44**, 2284–2292 (2005).
51. K. Palczewski, G protein-coupled receptor rhodopsin. *Annu. Rev. Biochem.* **75**, 743–767 (2006).
52. R. K. Sunahara, C. W. Dessauer, A. G. Gilman, Complexity and diversity of mammalian adenylyl cyclases. *Ann. Rev. Pharmacol. Toxicol.* **36**, 461–480 (1996).
53. D. Willoughby, D. M. Cooper, Organization and Ca2+ regulation of adenylyl cyclases in cAMP microdomains. *Physiol. Rev.* **87**, 965–1010 (2007).
54. R. Sadana, C. W. Dessauer, Physiological roles for G protein-regulated adenylyl cyclase isoforms: Insights from knockout and overexpression studies. *Neurosignals* **17**, 5–22 (2009).
55. A. Alfonso, K. Grundahl, J. S. Duerr, H. P. Han, J. B. Rand, The *Caenorhabditis elegans unc*-17 gene: A putative vesicular acetylcholine transporter. *Science* **261**, 617–619 (1993).
56. J. R. Johnson *et al.*, Ethanol stimulates locomotion via a Galphas-signaling pathway in IL2 neurons in *Caenorhabditis elegans*. *Genetics* **207**, 1023–1039 (2017).
57. O. A. Masseck *et al.*, Vertebrate cone opsins enable sustained and highly sensitive rapid control of Gi/o signaling in anxiety circuitry. *Neuron* **81**, 1263–1273 (2014).
58. E. S. Boyden, A history of optogenetics: The development of tools for controlling brain circuits with light. *F1000 Biol. Rep.* **3**, 11 (2011).
59. K. Deisseroth, Optogenetics. *Nat. Met.* **8**, 26–29 (2011).
60. P. Hegemann, G. Nagel, From channelrhodopsins to optogenetics. *EMBO Mol. Med.* **5**, 173–176 (2013).
61. K. Deisseroth, P. Hegemann, The form and function of channelrhodopsin. *Science* **357**, eaan5544 (2017).
62. S. J. Husson *et al.*, Microbial light-activatable proton pumps as neuronal inhibitors to functionally dissect neuronal networks in *C. elegans*. *PLoS One* **7**, e40937 (2012).
63. B. N. Armbruster, X. Li, M. H. Pausch, S. Herlitze, B. L. Roth, Evolving the lock to fit the key to create a family of G protein-coupled receptors potently activated by an inert ligand. *Proc. Natl. Acad. Sci. U.S.A.* **104**, 5163–5168 (2007).
64. B. R. Conklin *et al.*, Engineering GPCR signaling pathways with RASSLs. *Nat. Met.* **5**, 673–678 (2008).
65. D. J. Urban, B. L. Roth, DREADDs (designer receptors exclusively activated by designer drugs): Chemogenetic tools with therapeutic utility. *Annu. Rev. Pharmacol. Toxicol.* **55**, 399–417 (2015).
66. P. Davis *et al.*, WormBase in 2022-data, processes, and tools for analyzing Caenorhabditis elegans. *Genetics* **220**, (2022).
67. E. Z. Macosko *et al.*, A hub-and-spoke circuit drives pheromone attraction and social behaviour in *C. elegans*. *Nature* **458**, 1171–1175 (2009).
68. S. Brenner, The genetics of *Caenorhabditis elegans*. *Genetics* **77**, 71–94 (1974).
69. H. J. Bailes, R. J. Lucas, Human melanopsin forms a pigment maximally sensitive to blue light (lambdamax approximately 479 nm) supporting activation of G(q/11) and G(i/o) signalling cascades. *Proc. Biol. Sci.* **280**, 20122987 (2013).
70. T. Nagata, M. Koyanagi, R. Lucas, A. Terakita, An all-trans-retinal-binding opsin peropsin as a potential dark-active and light-inactivated G protein-coupled receptor. *Sci. Rep.* **8**, 3535 (2018).
71. s. de la Fuente, R. I. Fonteriz, P. J. de la Cruz, M. Montero, J. Alvarez, Mitochondrial free [Ca(2+)] dynamics measured with a novel low-Ca(2+) affinity aequorin probe. *Biochem. J.* **445**, 371–376 (2012).